

General Disclaimer

One or more of the Following Statements may affect this Document

- This document has been reproduced from the best copy furnished by the organizational source. It is being released in the interest of making available as much information as possible.
- This document may contain data, which exceeds the sheet parameters. It was furnished in this condition by the organizational source and is the best copy available.
- This document may contain tone-on-tone or color graphs, charts and/or pictures, which have been reproduced in black and white.
- This document is paginated as submitted by the original source.
- Portions of this document are not fully legible due to the historical nature of some of the material. However, it is the best reproduction available from the original submission.

NASA CR-156738

Prepared for
National Aeronautics and
Space Administration
Goddard Space Flight Center
Greenbelt, Maryland 20771

Quantitative mapping of rainfall rates over the oceans utilizing Nimbus-5 ESMR data

(NASA-CR-156738) QUANTITATIVE MAPPING OF
RAINFALL RATES OVER THE OCEANS UTILIZING
NIMBUS-5 ESMR DATA Final Report, Jan. 1975
- Nov. 1976 (Environmental Research and
Technology, Inc.) 30 p HC A03/MF A01

N78-22545

Unclas
G3/47 14717

Prepared by
Mirle S. V. Rao
William V. Abbott



REF: 076-011-ML-1704

ERT Document No. P-516

November 30, 1976

Mr. John Theon
Code 911
Goddard Space Flight Center
Greenbelt, Maryland 20771

Subject: Final Report - Contract No. NAS5-21908

Dear Mr. Theon:

Enclosed please find ten (10) copies of the final report for Contract No. NAS5-21908, entitled "Quantitative Mapping of Rainfall Rates over the Oceans Utilizing Nimbus-5 ESMR Data". This report deals with the use of ESMR in deducing estimates of precipitation amounts over the oceans as well as the relation of these data to available ground truth information and to large scale processes in the atmosphere.

Additional single copies of this report will be submitted separately to the following, to meet the contract specifications:

- Mr. J.J. Gentilini, Contracting Officer, Code 289, GSFC
- Publications Branch, Code 251, GSFC
- Patent Counsel, Code 204, GSFC

We understand that delivery of the final report completes our obligations under this contract.

Environmental Research & Technology, Inc. (ERT) has greatly appreciated the opportunity to perform this study and looks forward to further participation in your programs.

Sincerely yours,

Kenneth R. Hardy
Kenneth R. Hardy
Manager, Earth Resources and
Atmospheric Physics Division

ERH/11s

cc: Mr. J.J. Gentilini, Contract Officer
Publications Branch
Patent Counsel

Enclosures

**ORIGINAL PAGE IS
OF POOR QUALITY**

1. Report No.	2. Government Accession No.	3. Recipient's Catalog No.	
4. Title and Subtitle Quantitative Mapping of Rainfall Rates over the Oceans Utilizing Nimbus-5 ESMR Data		5. Report Date November 1976	
		6. Performing Organization Code	
7. Author(s) Hirle S.V. Rao and William V. Abbott		8. Performing Organization Report No. P-516	
		10. Work Unit No.	
9. Performing Organization Name and Address Environmental Research & Technology, Inc. 626 Virginia Road Concord, MA 01742		11. Contract or Grant No. NAS5-21905	
		13. Type of Report and Period Covered Final Report (Type III) January 1973 through Nov. 1976	
12. Sponsoring Agency Name and Address National Aeronautics & Space Administration Washington, D.C. 20546		14. Sponsoring Agency Code	
		15. Supplementary Notes Technical Officer: John Theon Goddard Space Flight Center Greenbelt, Maryland 20771	
16. Abstract The Electrically Scanning Microwave Radiometer (ESMR) data from the Nimbus-5 satellite was used to deduce estimates of precipitation amount over the oceans. An atlas of the global oceanic rainfall was prepared and the global rainfall maps analyzed and related to available ground truth information as well as to large scale processes in the atmosphere. It was concluded that the ESMR system provides the most reliable and direct approach yet known for the estimation of rainfall over data sparse, wide oceanic regions.			
17. Key Words (Suggested by Author(s)) Rainfall Mapping Meteorology Ocean Rainfall ESMR Data		18. Distribution Statement Unclassified-Unlimited	
19. Security Class. (of this report) Unclassified	20. Security Class. (of this page) Unclassified	21. No. of Pages 26	22. Price*

TABLE OF CONTENTS

	Page
1. INTRODUCTION	1
2. THE TRAILER EXPERIMENT	2
3. THEORETICAL APPROACH	8
4. GENERATION OF MAPS	10
5. COMPARISONS TO CONVENTIONALLY ACQUIRED DATA	11
6. MOVEMENT OF RAIN PATTERNS	12
7. CIRCULATIONS AND INTERACTIONS	20
8. LATENT HEAT	22
9. MOVEMENT OF ICE AND THE ICE LINE	23
10. LIMITATIONS AND POSSIBLE IMPROVEMENTS	24
11. GATE AREA MAPS	25
REFERENCES	26

ORIGINAL PAGE IS
OF POOR QUALITY

1. INTRODUCTION

Our knowledge of rainfall occurring over the oceans which cover almost three-fourths of the earth's surface has always been limited by a lack of data. The principal objective of this program was to increase this knowledge-base by estimating rain-rates over the oceans, utilizing data from the Electrically Scanning Microwave Radiometer (ESMR) aboard the Nimbus-5 satellite, and to examine oceanic rainfall climatology.

The basis of the investigation is the selective response to liquid water in the atmosphere of ESMR, operating at 19.35 GHz (bandwidth 250 MHz). Because the emissivity of water, ϵ_w , in the vicinity of 19 GHz is low (≈ 0.4) and inversely proportional to the thermodynamic temperature, T_w , whereas the brightness temperature as observed by ESMR is proportional to the product, $\epsilon_w T_w$, the oceans provide a convenient, nearly uniform background for the satellite-borne radiometer. With the advantages of a) selective response to rain, and b) background uniformity, the ESMR system provides the most reliable and direct approach yet known for the estimation of rainfall over wide oceanic regions.

In this study, it was first important to obtain an appropriate calibration curve to convert LSR brightness temperature data to rain-rates. For this purpose, a specially designed ground-based experiment was performed over a period of several months, in a trailer at NASA Goddard Space Flight Center. (Two micro wave radiometers with center frequencies of 19.35 GHz and 37.0 GHz were mounted viewing upwards at a 45 degree zenith angle. The relevant parameters of each are summarized in Table 1.

TABLE 1
RADIOMETER PARAMETERS

Parameter	Radiometer 1	Radiometer 2
Frequency	19.35 GHz	37.0 GHz
Wavelength	1.55 cm	0.81 cm
Bandwidth	400 MHz	400 MHz
E-plane Beamwidth	6.5 degrees	6.5 degrees
H-plane Beamwidth	9.0 degrees	9.0 degrees

(Rectangular cross-section, horn-type antennas were mounted) with the electric field vector horizontal so that the E-plane antenna gain pattern, having larger sidelobes than the H-plane gain pattern, caused a minimum variation in elevation throughout the field of view. The antenna horns were shielded from direct rainfall by a wooden housing open on one side. They were protected against wetting from blowing rain by placing a plastic wrapping across their apertures and a blower which directed a stream of dry air across the plastic wrap. (The receivers were connected in turn for a period of 15 seconds each to a) their respective antennas, b) a reference cold load, and c) a reference warm load. The outputs were fed to a small computer which calculated both of the mean brightness temperatures for the 15 seconds when the radiometers were sensing the radiation from the antennas (separately at 19.35 GHz and 37.0 GHz) and printed out the results at intervals of 0.8 minutes.)

(Two rain gauges of different types were used to measure the rainfall intensities concurrent with the radiometer observations. The first was a conventional tipping bucket rain gauge located adjacent to the antenna housings. The number of times the bucket tipped was registered by a counter and recorded on the computer print-out alongside the radiometer readings. The second was the recently developed (Raymond and Wilson, 1974) electronic rain intensity gauge with a one-second response time, located at a horizontal distance of 23.5 meters away from the radiometers in the direction of the antenna beams.) In this type of rain gauge, measurement is made of the ratio of the resistance of rain water flowing in a trough between two electrodes spaced along the trough (R_1), to the resistance of the same rain water in a chamber of fixed geometry (R_2). Since R_1 varies as the resistivity divided by the cross sectional area of the flowing water while R_2 varies only as the resistivity, R_2/R_1 is independent of resistivity and is proportional to the cross-sectional area; i.e., it is related only to the rate of flow. Both rain gauges were calibrated against directly measured flow rates and both had 91 cm funnel apertures.

(Data were collected with this arrangement from June through September 1974.) On all occasions on which data were taken, the freezing level was 4 ± 0.5 km. With the aid of the laboratory calibration curve, the voltage records on chart paper were translated to rainfall rates. The brightness temperatures of the 19.35 GHz and 37.0 GHz radiometer systems were tabulated against rainfall intensities. For this purpose, only those occasions when the rain-rate and temperatures were steady for two minutes or more were considered, in order to avoid excessive scatter in the data. The observations were then grouped under 18 categories according to rainfall rate intervals:

- 10 categories at 1 mm hr^{-1} intervals from 0 to 10 mm hr^{-1} ,
- 5 categories at 2 mm hr^{-1} intervals from 10 to 20 mm hr^{-1} ,
- 2 categories at 10 mm hr^{-1} intervals from 20 to 40 mm hr^{-1} ,
- and
- one category greater than 40 mm hr^{-1} .

In each category, (the mean and standard deviation were calculated separately with respect to brightness temperature (\bar{T}_B and σ_{T_B}) and rainfall (\bar{R} and σ_R). Figure 1 shows the result for 19.35 GHz and Figure 2 that for 37.0 GHz. In both figures, the vertical lines and horizontal lines are equal in length to 2 standard deviations.

(Approximating the radiometric effect in this case by an isothermal, non-scattering layer of absorber at a temperature of 273°K, these upward viewing data were converted to what would have been observed by the ESMR if ^{it were viewing a water surface} this atmosphere were over water. These data are presented in Figure 3.)

ORIGINAL PAGE IS
OF POOR QUALITY

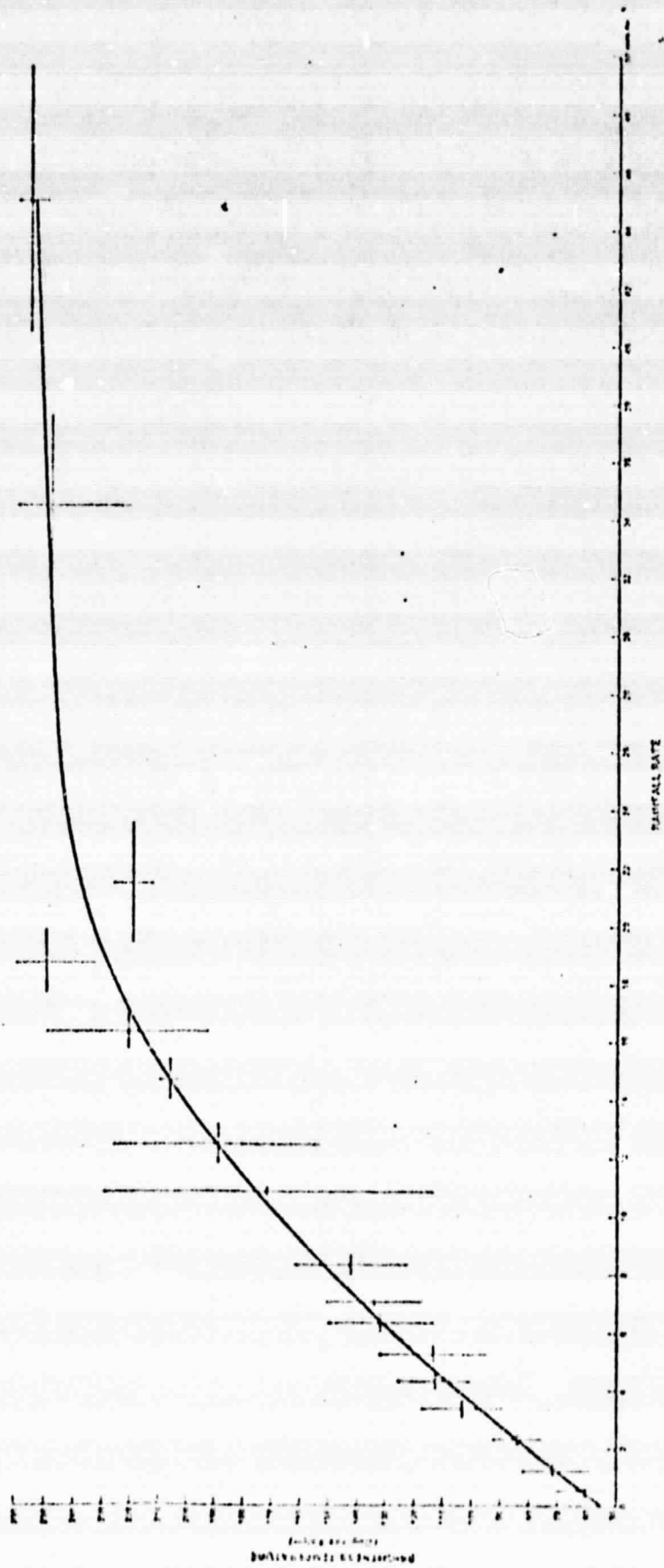


Figure 1 Trailer Experiment Results for 19.35 GHz Sensor Looking Up at a 45° Zenith Angle

ORIGINAL PAGE IS
OF POOR QUALITY

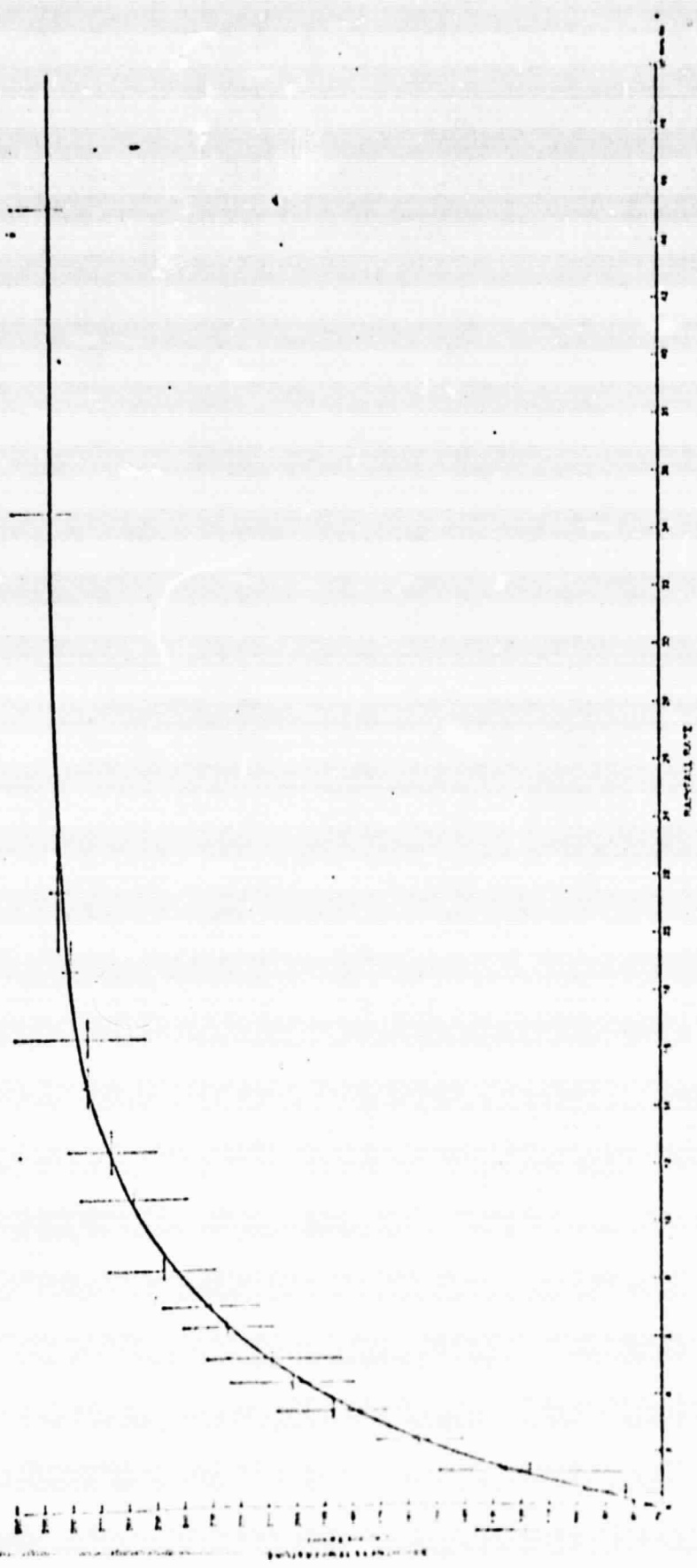


Figure 2 Trailer Experiment Results for 37.0 GHz Sensor Looking Up at a 45° Zenith Angle

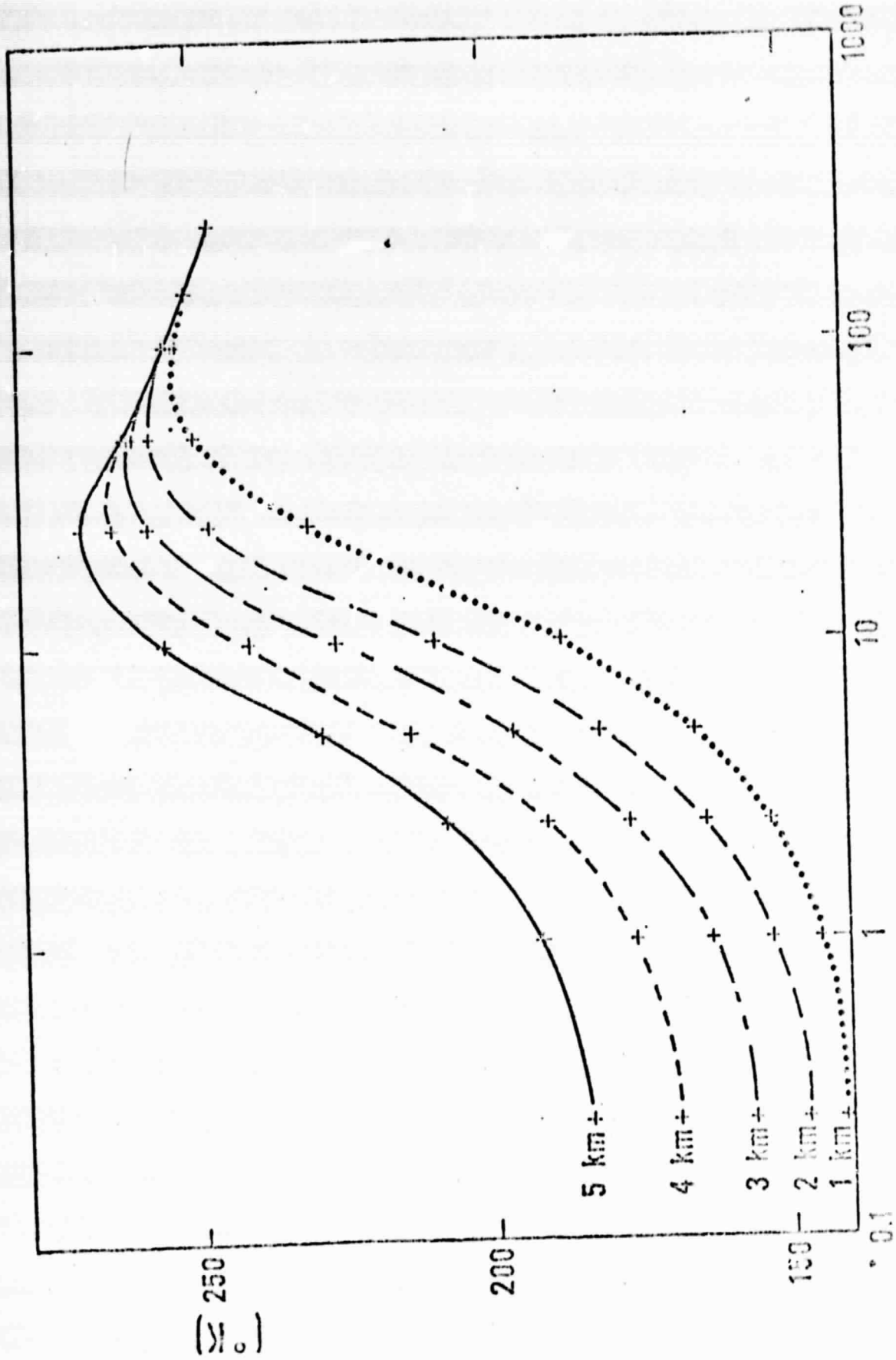


Figure 4 Relationship Between Brightness Temperature and Rainfall Rate at Different Freezing Levels

4. GENERATION OF MAPS

Using the calibration curves, an attempt was made to map oceanic rainfall on a global scale. Note that in actual practice, several corrections and modifications to the curves were necessary. The principal modification resulted from the realization that the sensitivity of the model to 273°K isotherm height was excessive (probably because supercooled water above the freezing level was not adequately considered in the model). Therefore, as a measure of compensation, a modified freezing-level pattern with only three steps of change over the globe had to be adopted to yield reasonable results. The uncertainty in Earth location caused problems close to land, which could be eliminated by disregarding data within 1 degree of coastlines and all significant islands. To avoid assigning noise attributable to factors such as surface wind, water vapor, and non-raining clouds as rainfall, all ESMR rates ranging from 1 mm hr^{-1} in the tropics to 2 mm hr^{-1} in high latitudes were ignored, and assumed to be noise. Finally, a small correction was made for the dependence of brightness temperature on the scanning angle, although this is relatively less important here than in studies on a smaller spatial or temporal scale. This correction to the brightness temperature was anywhere from 0 to 2°K.

The rain-rate data were averaged first over a 1-degree latitude by 1-degree longitude grid and then again over the 4-degree latitude by 5-degree grid used by the staff of the Goddard Institute of Space Studies (GISS) in their general circulation model and Global Atmospheric Research Program (GARP) studies (GARP-GISS grid). If, in any grid-cell, land predominated (> 75 percent), rainfall in the cell was ignored.

Proceeding as above, maps were generated for the period December 11, 1972 (i.e., the day of launch), through the end of February 1975 on a weekly, monthly, and seasonal basis. Annual averages for 1973 and 1974 were also calculated and charted. These maps have been compiled in the form of an Atlas (Rao, Abbott and Theon, 1976).

ORIGINAL PAGE IS
OF POOR QUALITY

5. COMPARISONS TO CONVENTIONALLY ACQUIRED DATA

Conventional rainfall data over the oceans is scarce and, therefore, insufficiently reliable for comparisons. As is well known, ship observations suffer from platform instability and sea-spray problems, and island reports do not represent the surrounding ocean because orographic effects modify the flow. Nevertheless, comparison with the best obtainable ground-truth data was attempted.

For example, a January 1973 map produced from ESMR data was compared to a map for the same month, produced by the Weather Service of the German Federal Republic, which includes some data over oceans apparently extracted from island and ship observations. These maps show broad agreement; both show principal areas of rainfall to be the Southwest Indian Ocean, the mid-Pacific and the North Atlantic. The magnitudes are also comparable; in the Southwest Indian Ocean, the rain rate in the maximum rain area is 0.4 mm hr^{-1} or 300 mm mo^{-1} (ESMR) compared to the monthly total of 450 mm (German data). In the mid-Pacific, the ESMR rain-rate figures in the rainiest areas compute to 600 mm mo^{-1} and 450 mm mo^{-1} , respectively, compared to 700 and 470 in the German data; and in the North Atlantic 370 mm mo^{-1} by ESMR vs. 200 in the German data.

As another exercise, the annual ESMR map for 1973 was compared to a climatological annual precipitation chart produced by Dr. Rudolf Geiger. The following regions show general agreement in the maxima: a) Eastern Indian Ocean and Bay of Bengal magnitudes computed at $2,200 \text{ mm yr}^{-1}$ (ESMR) compared to 2000 to 3000 on Geiger's chart; b) China Sea at $3,600 \text{ mm yr}^{-1}$ (ESMR) compared to 2000 (Geiger); c) Equatorial Pacific and Atlantic (i.e., the Intertropical Convergence Zone (ITCZ) at $1,800 \text{ mm yr}^{-1}$ (ESMR) compared to 2,000 (Geiger); and d) Gulf of Alaska $1,800 \text{ mm yr}^{-1}$ (ESMR) compared to 2,000 (Geiger). Furthermore, the regions of minima are strikingly similar. They are the Northwest Arabian Sea and the west coasts of California, North Africa, Australia, South America, and South Africa (the last with ESMR rain rates of 400 mm yr^{-1} vs. Geiger's less than 100).

6. MOVEMENT OF RAIN PATTERNS

Monthly maps of rainfall rates are suitable for the study of displacement of rain belts, and of changes in the intensity of the ITCZ from month to month. Furthermore, the structure of the ITCZ or at least the associated rain pattern - a forking in the Pacific with the southern limb merging as it runs southeast with the polar front - is of interest. This pattern throws further light on the observations of Seelye (1950) of a dry zone near the Ellice Islands in the mid-Pacific.

In this investigation, a detailed study of the progress of the rain belts separately in each of the three major oceanic areas of the world, the Pacific, Atlantic, and Indian Oceans was undertaken. The results of the study are presented in graphical form in Figures 5 through 8, which depict the zonally averaged rainfall over the oceans. The rainfall rate over the oceans appears to be lower in the Southern Hemisphere than in the Northern Hemisphere, particularly in the Atlantic. There appears to be a regular evolution of the maxima in the curves with the progression of the seasons.

In the Pacific (Figure 5), the ITCZ shows a general displacement to the north of the Equator. The ITCZ is perhaps more sharply defined and its seasonal movement more pronounced in the Atlantic (Figure 6). The polar front near 40°N is active from September through November, whereas its complement in the Southern Hemisphere, which is apparently weaker, manifests its greatest activity from March through May. Figure 7 shows two main crests in the Indian Ocean, the one at higher latitudes growing at the expense of the other at lower latitudes as the monsoon advances and vice versa as it retreats. Figure 8 represents the global integrated picture.

The Southwest Monsoon affects the lives of millions of people in Indian and Southeast Asia. The weekly maps for May 29 through June 14, 1973 (Figures 9a, b, and c), portray the onset of the monsoon; the two weekly maps for October 8 through October 21, 1973 (Figures 10a and b), show the retreat of the monsoon. According to the official Indian weather summary, the date of onset of the monsoon to peninsular India,

ORIGINAL PAGE IS
OF POOR QUALITY

in 1973, was June 10, and the date of withdrawal from the main part of that region was October 16. This closely corresponds to the LSMR data. Thus, these maps indicate the feasibility of producing daily maps to monitor the advance of the monsoon from the Indian Ocean towards the Southeast Asian land-mass and to predict its onset and later development.

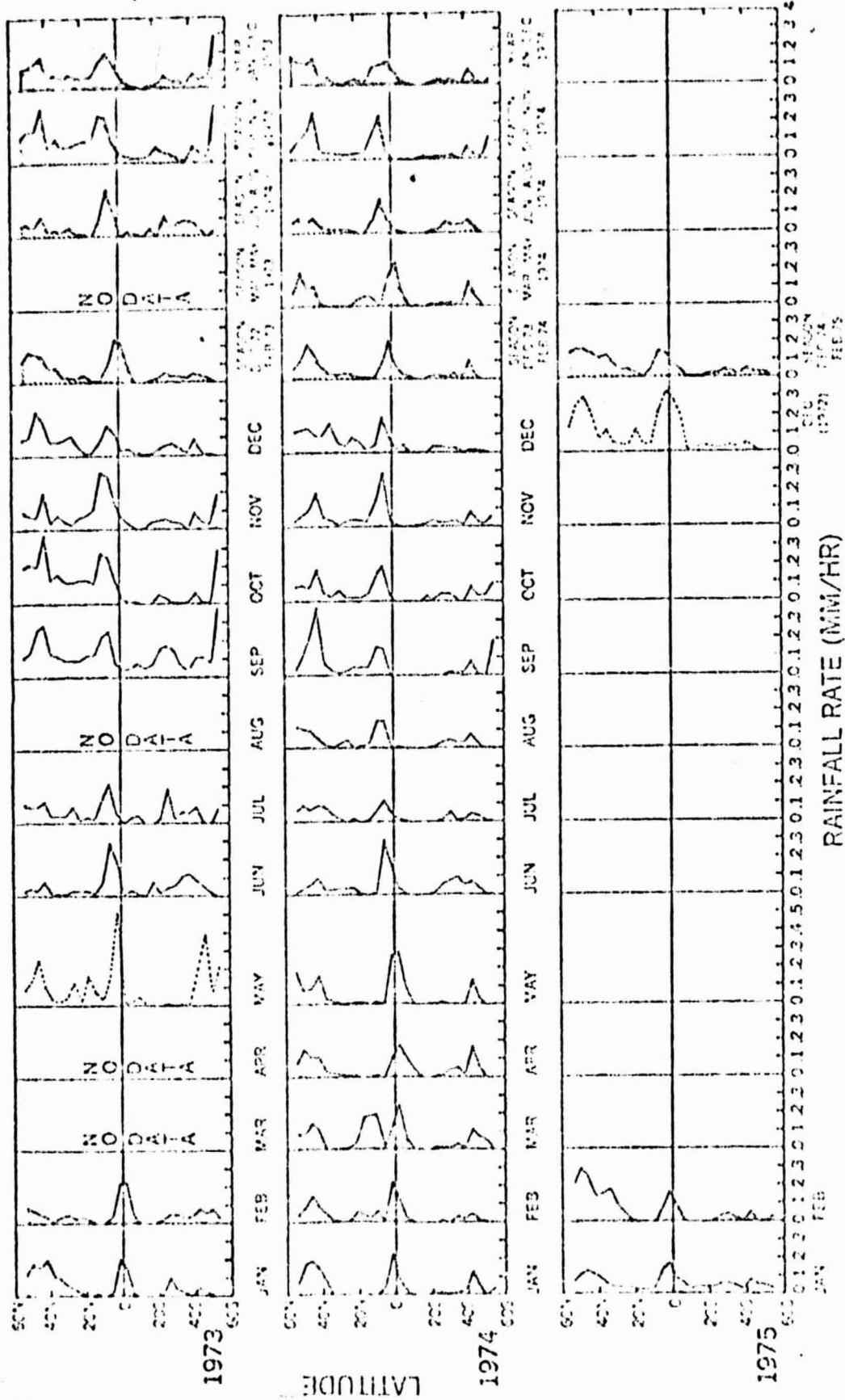
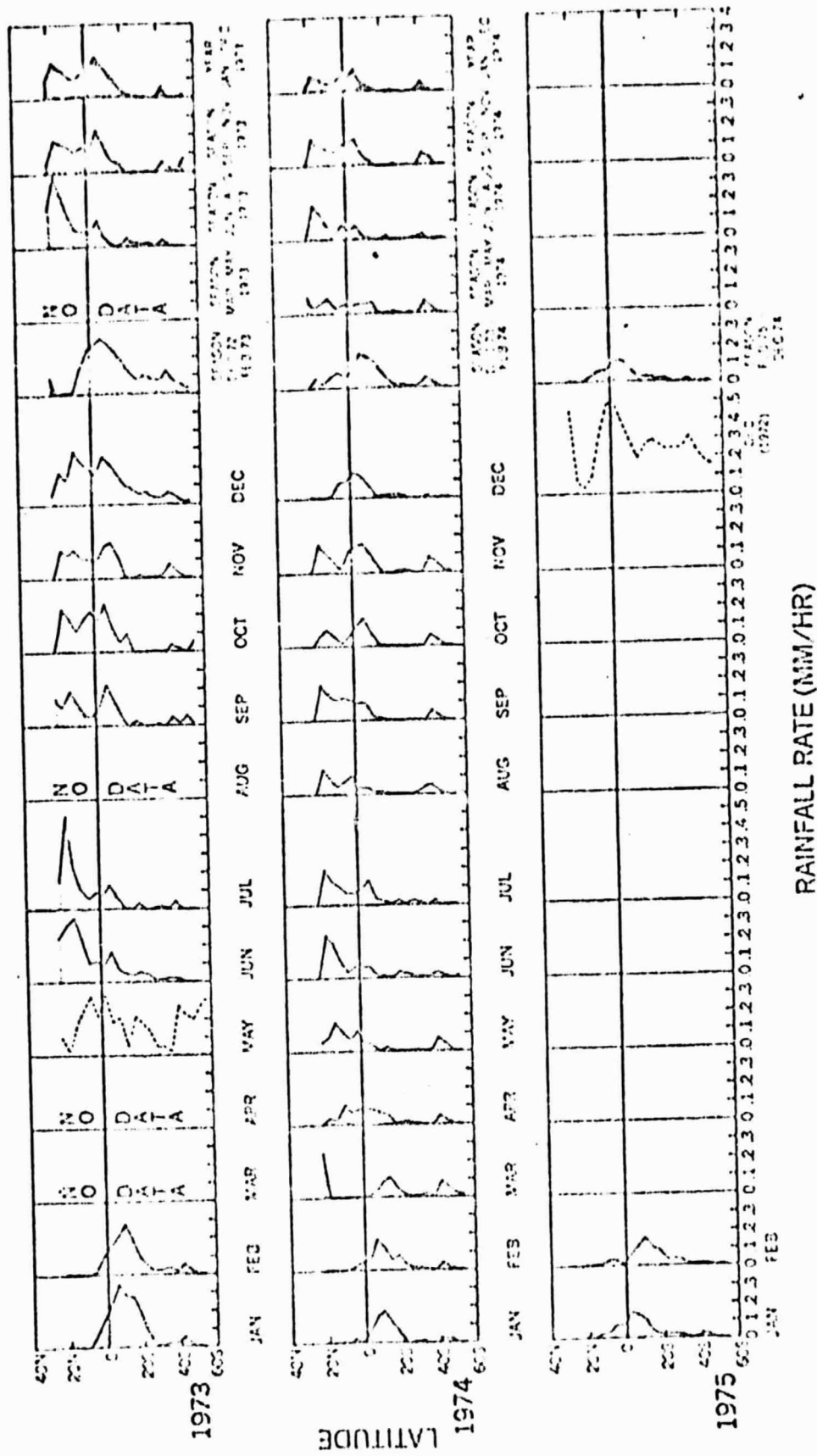


Figure 6 Zonally Averaged Rainfall Rate from ESMR Data - Atlantic Ocean



(NOTE: BROKEN LINES REPRESENT CURVES BASED ON INADEQUATE DATA)

Figure 7 Daily Averaged Rainfall Rate from ESMR Data - Indian Ocean

ORIGINAL PAGE IS OF POOR QUALITY

29-31 MAY

1-7 JUNE

8-14 JUNE

Reinfall Rate
(mm/hr)

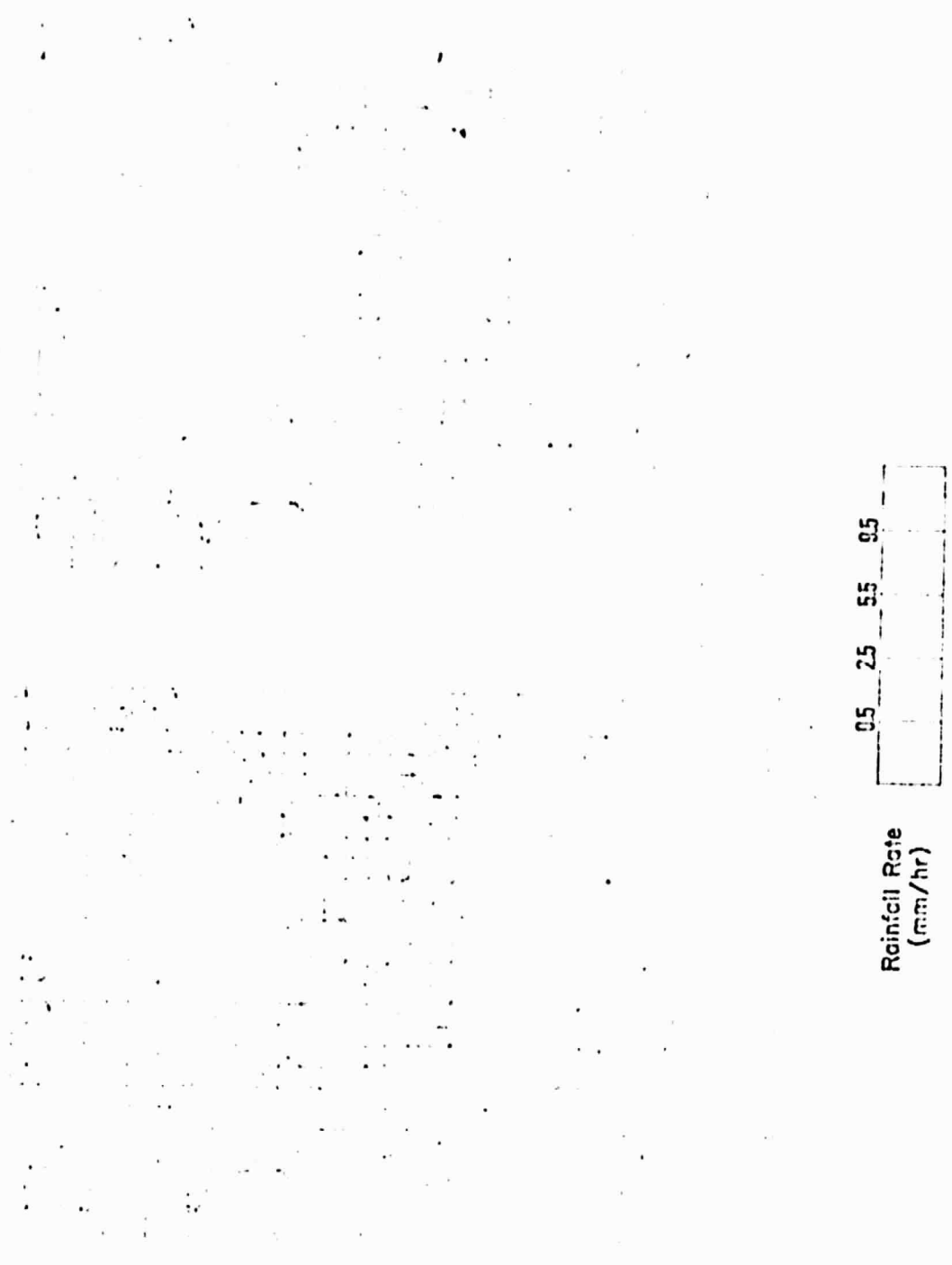
05 25 55 95

Figure 9 1975 Monsoon Onset as Portrayed by the ESNR Data

ORIGINAL PAGE IS
OF POOR QUALITY

0117 UGI.

13-21 UGI.



Rainfall Rate
(mm/hr)

0.5	2.5	5.5	9.5
-----	-----	-----	-----

Figure 10 1975 Monsoon Retreat as Portrayed by the ESRR Data

7. CIRCULATIONS AND INTERACTIONS

By careful inspection, it is possible to infer local circulations from the rain patterns in the oceanic areas. For example, in the Pacific, interannual comparison between the austral summers of 1972-73 and 1973-74 reveal that they are meteorologically very different seasons. In January 1973, ESMR recorded that intense rainfall occurred over a wide region along the Equator and to the south of it in the mid-Pacific, which was absent in the January 1974 data (Figures 11a and b). The extensive and heavy rain in January 1973 must be associated with pronounced convection and a large-scale rising current. This precipitation, together with the dry region of subsidence off the coast of South America, leads to the concept of a possible important local variation in the Hadley cell circulation. This could very likely be linked with the relaxation in upwelling, commonly known as the El Niño phenomenon, with its disastrous effect on the plankton and fish in the waters of the Pacific off the west coast of South America.

JANUARY 1973

JANUARY 1974

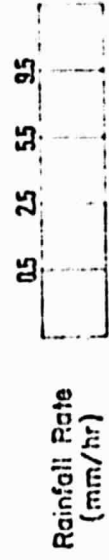
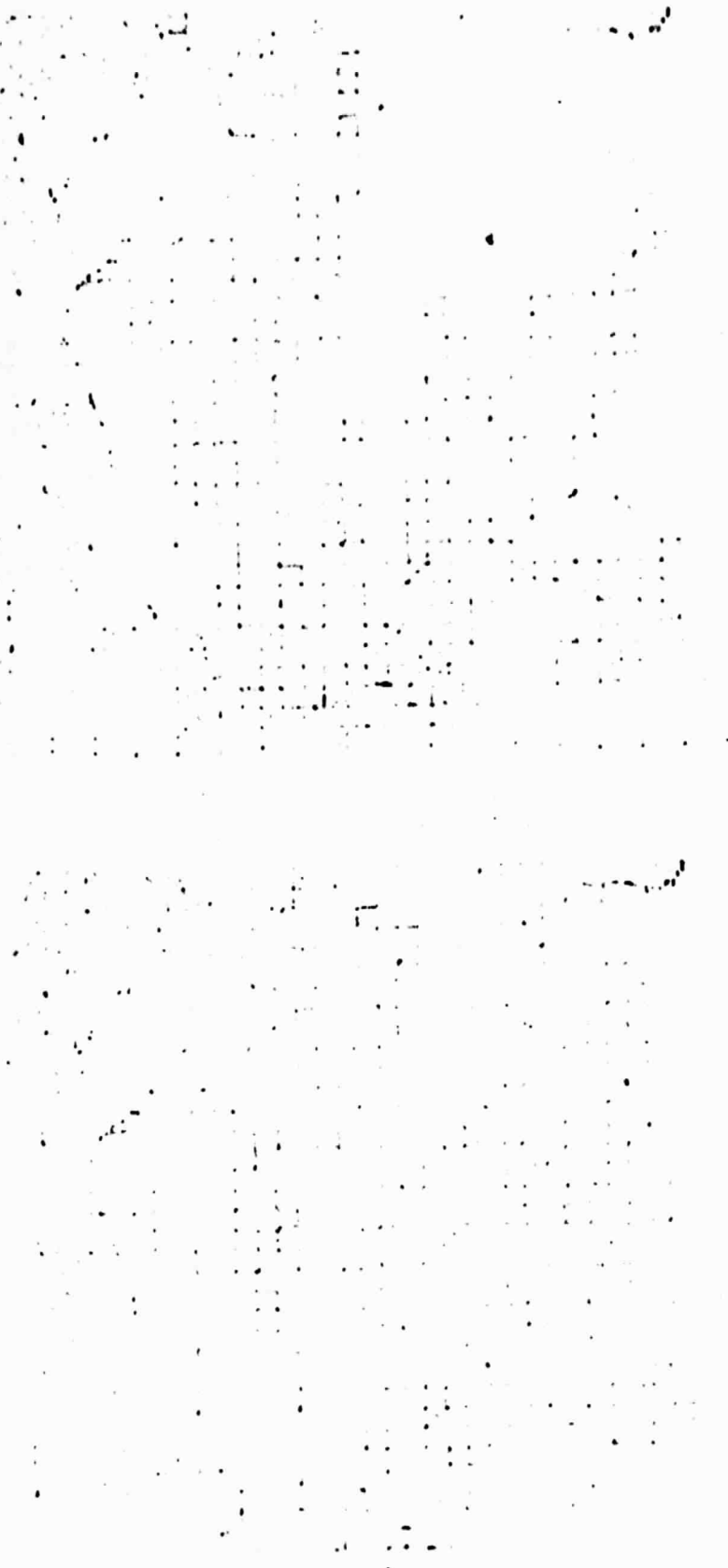


Figure 11 Global Oceanic Rainfall Rates for Two Consecutive Januarys

ORIGINAL PAGE IS
OF POOR QUALITY

8. LATENT HEAT

The rate of latent heat release (in kilojoules sec^{-1}) in each of the GARP-GISS LSMR grid cells is also available. To prevent overcrowding and confusion, these figures have not been shown on the maps in this report, although they are available in the printouts for the weekly, monthly, seasonal, and annual periods (archived at Goddard Space Flight Center). The latent heat data, together with rainfall data, provide useful inputs to numerical models and make possible a better understanding of the planetary energy and water budgets.

9. MOVEMENT OF ICE AND THE ICE LINE

Data at latitudes poleward of 52 degrees are often contaminated by sea ice. This shortcoming could be turned to advantage. The standard ESMR mapped data representations utilize x's at high latitudes to indicate the position of sea ice. By resorting to a finer grid, the displacement of the ice line (especially in the Southern Hemisphere) can be followed from day to day or week to week, according to requirements. P. Gloersen and H. J. Zwally (GSFC) are preparing an ice-boundary atlas based on ESMR data. The U. S. Navy Fleet Weather Facility uses these data operationally for ice mapping. It should be mentioned that in the present maps the x's are changed to 0 at very high latitudes where the freezing level is zero and there is no precipitation in liquid form.

10. LIMITATIONS AND POSSIBLE IMPROVEMENTS

The mapping procedure adopted here is open to criticism in many respects. For example, no allowance has been made at the present stage for possible diurnal variations, because there is no generally accepted pattern of diurnal variation over the oceans. More importantly, it is not easy to conceive clearly of the physical causes or mechanisms that could bring about diurnal variation over the open sea, although this is not to say that such variation does not exist. Because of this and several other imperfections, no claim is made for reliability in absolute values of rain rate better than a factor of 2, although in a relative sense, the values are much more dependable when changes are considered.

Several refinements for improving the results are possible. The principal ones are: a) improving the model by adequately considering the liquid water above the freezing level, b) improving the ephemeris and spacecraft attitude and their use to minimize Earth-location error, and c) investigating and correcting the effects of diurnal variation, if significant.

ORIGINAL PAGE IS
OF POOR QUALITY

11. GATE AREA MAPS

At the request of the U. S. Project Office, a set of 1-degree latitude by 1-degree longitude rainfall charts were generated. These charts covered the area bounded by 10°S to 25°N and 15°E to 95°W and consisted of separate daytime and nighttime observations for each of the days of the Gate experiment, viz., 15 June through 30 September 1974.

Preliminary statistical analysis of these rainfall observations was also made. The figures reveal that rainfall over oceans near local noon is greater than that near local midnight. The ratio of the day to night frequency of occurrence is 1.41, while the day to night ratio of rainfall intensity is 1.72. A possible component of this variation due to instrumental calibration problem (residual effect of the solar cycle on the orbiting ESMR circuitry) needs to be investigated and removed before the net diurnal variation is assessed.

REFERENCES

- Rao, M. S. V., W. V. Abbott and J. S. Theon, 1976: "Satellite-Derived Global Oceanic Rainfall Atlas (1973 & 1974)," NASA/GSFC X-911-76-116.
- Raymond, D. J. and K. Wilson, 1974: "Development of a New Rainfall Intensity Gauge," J. Applied Met., 13, pp. 180-182.
- Seelye, C. J., 1950: "Rainfall and its Annual Variability over the Central and Southwestern Pacific". New Zealand J. Sci. Tech., B52, pp. 11-24.
- Wilheit, T. T., M. S. V. Rao, T. C. Chang, E. G. Rodgers, and J. S. Theon, 1975: "A Satellite Technique for Quantitatively Mapping Rainfall Rates over the Oceans," NASA/GSFC TM X-70904, 1972, p. 28.